PHILOSOPHICAL TRANSACTIONS OF THE ROYAL SOCIETY A MATHEMATICAL, PHYSICAL & ENGINEERING SCIENCES

Bow–like free surfaces under gravity

E. O. Tick and A. J. Roberts

Phil. Trans. R. Soc. Lond. A 1997 **355**, 665-677
doi: 10.1098/rsta.1997.0032

Bow-like free surfaces under gravity

By E. O. Tuck[1] and A. J. Roberts[2]

[1]*Department of Applied Mathematics, The University of Adelaide, South Australia 5005, Australia*

[2]*Department of Mathematics and Computing, University of Southern Queensland, Toowoomba, Queensland 4530, Australia*

The nonlinear free-surface flow near the extreme bow of a ship is a classical hydrodynamic example of a violent surface motion. The nature of these bow flows is discussed, and previous studies on them are reviewed, with emphasis on splashes and their elimination. Some new examples are provided of bow-like flows without splashes that can be computed by inverse means. In effect, the shape of the free surface is given, and the bow shape that generates this free surface is determined. This exact solution-generating procedure, which dates at least from 1901, is in principle capable of being turned into a practical design tool. Although this point has not been yet reached, some of the examples given here are not unlike the flow at the bow of a bluff ship.

1. Introduction

The flow at the bow of a ship is an important example of a highly nonlinear large-displacement free-surface flow. Most ship bows create a splash, sometimes massive and overturning directly in front of the ship to create a large foaming zone, as with the bluff bow of a barge or supertanker, but sometimes thin and fountain-like, rising high and falling sideways with little apparent effect on the water ahead, as with a fine yacht bow. The insult caused to the calm still water ahead of a ship on suddenly meeting a rapidly moving object seems (almost) always to produce a splash.

The nonlinear nature of bow splashes makes for a very difficult analytical and computational task if one attempts to provide a theoretical description of the flow about a ship. Success in modelling bow splashes would be of some technological interest; splashes are undesirable on many grounds, being a source of drag and noise, to name just two of these grounds. This is so particularly for bluff bows, where the flow is approximately two-dimensional.

It is only very recently (Dias & Vanden-Broeck 1993) that some limited progress has been made in computing actual two-dimensional splashing flows. One difficulty with strictly two-dimensional bow flows is that after the splash is generated and rises into the air, there is nowhere safe for it to go when it later falls under gravity, and artificial means must be adopted, like letting it fall freely for ever on another Riemann sheet (see Dias & Tuck 1993; Jenkins 1994). This is necessary to avoid having to model what really happens in practice, but what is virtually impossible to treat mathematically, namely violent contact of the splash with the water ahead of the bow to produce a foaming rotational 'forward wake' (Mori 1984). Another

Phil. Trans. R. Soc. Lond. A (1997) **355**, 665–677
Printed in Great Britain

possibility is to divert the splash, e.g. over the top of the bow, as in Tuck (1997); some other artificial splash-absorbers are discussed in Tuck (1991).

Much more progress can be made mathematically and computationally by ignoring the splash, or by assuming that the bow shape is somehow such that there really is no splash. At this stage it is still somewhat of a mystery how some of the very successful recent numerical codes (e.g. Raven 1992) for flow about actual three-dimensional ships can appear to be numerically convergent in spite of the fact that they assume no splash. It is probable that in these cases the splash occurs on a length scale that is small compared to the coarse numerical grid used; if the grid were refined further, the need for detailed splash analysis might become apparent (see Roberts 1987). Attempts are being made (Scullen & Tuck 1995) to develop codes which will eventually allow such fine flow details to be incorporated.

Returning to the two-dimensional case, the issue of whether a bow flow can ever be without a splash has received some attention recently. Farrow & Tuck (1995) have shown that there can be splashless bow flows providing that the initial contact between free surface and bow is tangential. This is an unlikely event to occur in practice, and can only happen if the 'bow' has a projection that slopes downward at the point of contact. This confirms results of Madurasinghe & Tuck (1986). For more conventional bluff bows, it is likely that the water rises to a stagnation point at attachment, and in that case Farrow & Tuck (1995) have provided numerical evidence to suggest that a splash must always occur, contradicting earlier somewhat less accurate work by Tuck & Vanden-Broeck (1984) and Madurasinghe (1988).

The linearized theory of two-dimensional planing surfaces (ships of small draft) provides some guidance in this bow-splash matter. That theory is analogous to thin-airfoil theory (Newman 1977, p. 179), and the bow splash is analogous to the leading-edge singularity of an airfoil. It is possible to design a specially cambered airfoil to have 'shock-free entry', i.e. to avoid the leading edge singularity, and this is equivalent to the tangential-attachment splash-free bow (Cumberbatch 1958). On the other hand, so long as there is a splash for a planing surface, it is a challenging task to correlate the size of the leading-edge singularity with the size of the splash, and there has been recent progress with that task (Tuck 1994, 1995).

In the remainder of the present paper, we turn to a very different procedure for computing splash-free bow flows. If there are such flows where the contact is via a stagnation point, then the free surface, while being a large displacement of the undisturbed plane, will nevertheless be a smooth continuous curve. In that case, surely it must be possible to determine the flow via inverse means, where the free surface is specified, and the bow shape that generates such a free surface is to be determined. Success in such an objective would provide a design procedure for an optimum bluff bow shape.

We now discuss such inverse procedures, but note immediately that we have not been able to determine any examples which are truly ship-like, in the sense of allowing for an effective uniform stream far from the body. Hence the existence of splashless bow flows with that far-field property and a stagnation point at attachment is still an open question.

2. Inverse methods

Inverse methods for generating steady two-dimensional irrotational flows that satisfy the free-surface boundary condition exactly, have a long history, surveyed by

Wehausen & Laitone (1960, pp. 736–740). Although equivalent methods have been rediscovered many times since, the first statement of the method appears to be due to Sautreaux (1901). The following is in the spirit of Sautreaux's original formulation; other formulations are obtainable by elementary changes of variable.

If $z = x + \mathrm{i}y$ is a complex coordinate and $f = \phi + \mathrm{i}\psi$ a complex velocity potential, irrotationality in an incompressible fluid demands that z and f be analytically related. We choose to seek $z = z(f)$ in $\psi \leqslant 0$, and write

$$z(f) = X(f) + \mathrm{i}Y(f), \tag{2.1}$$

where $X(f)$, $Y(f)$ are analytic functions connected for all f by

$$X'(f)^2 + Y'(f)^2 + [2gY(f)]^{-1} = 0. \tag{2.2}$$

for some constant g. If X and Y are real and g denotes the acceleration of gravity, equation (2.2) is the free-surface boundary condition; however, this is not always the case.

More generally, (2.1) is a somewhat arbitrary decomposition of z into two parts, and does not necessarily imply that X and Y are real and imaginary parts of z, respectively. However, suppose they are real on some or all of the streamline $\psi = 0$. That is, suppose that there exists a range of real values of ϕ such that $X(\phi)$ and $Y(\phi)$ are both real. Then, for such ϕ values, (2.2) guarantees that the pressure (excess over atmospheric, with ρ the constant fluid density)

$$\begin{aligned} p &= -\rho\left[\frac{1}{2}\left|\frac{\mathrm{d}f}{\mathrm{d}z}\right|^2 + gy\right] \\ &= -\tfrac{1}{2}\rho\left[\left(X'(f)^2 + Y'(f))^2\right)^{-1} + 2gY(f)\right] \end{aligned} \tag{2.3}$$

vanishes when $f = \phi$ is real. Thus, any choice of $X(f)$ and $Y(f)$ satisfying (2.2) generates an exact free surface whenever both are real. The converse is not necessarily true.

Most authors (in effect) fix $Y(f)$, and use (2.2) as an explicit quadrature formula for $X(f)$, namely

$$X(f) = \int [-Y'(f)^2 - (2gY(f))^{-1}]^{1/2}\,\mathrm{d}f. \tag{2.4}$$

However (c.f. Vanden-Broeck *et al.* 1978), (2.2) may also be written

$$\left(\frac{\mathrm{d}Y}{\mathrm{d}f}\right)^2 + \frac{1}{2gY} = -X'(f)^2, \tag{2.5}$$

and interpreted as a nonlinear first-order ordinary differential equation for $Y = Y(f)$, given $X(f)$. In either method, (2.4) or (2.5), there is a degree of freedom associated with the additive constant in (2.4) or the initial condition in (2.5). However, the additive constant in (2.4) represents a mere shift in origin and can be ignored, whereas a more complicated range of possibilities exists as we vary the initial condition to be used in solving the differential equation (2.5).

Portions of the streamline $\psi = \psi_0$ on which X and Y are not both real can be interpreted as a solid body, to which the free part of the streamline is attached. In this paper we shall be concerned with streamlines $\psi = 0$, of which a portion (generally $\phi > \phi_0$ for some ϕ_0) is free, and the remainder, $\phi < \phi_0$, is solid.

Furthermore, in most cases both the free and solid portions will be asymptotically straight lines, i.e.

$$y \to (\tan\theta_\pm)x \text{ as } \phi \to \pm\infty, \tag{2.6}$$

where $\theta_\pm$ are the angles these lines make with the x-axis. Indeed, in most cases, our examples have

$$\theta_+ - \theta_- = \tfrac{2}{3}\pi, \tag{2.7}$$

and

$$z(f) \to A\mathrm{e}^{\mathrm{i}\theta_+} f^{2/3}, \quad \text{as } |f| \to \infty, \tag{2.8}$$

for some real positive constant A. These flows thus appear as flows in a 120° sector, one arm of which is solid and the other free. However, the sector is distorted in various ways near its corner (c.f. Vanden-Broeck & Tuck 1994), and we are particularly interested in the manner in which the free surface joins the body, as a model of the corresponding attachments at the bow and stern of a ship.

3. Two-thirds power

The choice

$$Y(f) = -Bf^{2/3}, \tag{3.1}$$

has been tried by a number of authors, with B constant. The only candidate free-surface streamline is $\psi = 0$, $\phi > 0$ and B is then necessarily real. Now (2.1) gives

$$X'^2 = \left(-\frac{4}{g}B^2 + \frac{1}{2gB}\right) f^{-2/3}, \tag{3.2}$$

so that X can be real on $f \in \mathbb{R}^+$ only if

$$0 < B < (9/8g)^{1/3}. \tag{3.3}$$

Defining

$$C = \left(\frac{9}{8gB} - B^2\right)^{1/2}, \tag{3.4}$$

then

$$X(f) = Cf^{2/3}, \tag{3.5}$$

that is

$$z(f) = (C - \mathrm{i}B)f^{2/3}. \tag{3.6}$$

Although, in principle, solutions with $C < 0$ are possible, these have 'water above air', and for physically acceptable flows we can confine attention to $C > 0$. Now as B ranges over the interval (3.3), C decreases from $+\infty$ to 0, and the free surface is the straight line

$$y = -(B/C)x, \tag{3.7}$$

which (as B varies from zero) varies from horizontal to vertical. Meanwhile, the remainder of the streamline $\psi = 0$ (i.e. that for $\phi < 0$) is the straight line at 120° to the free surface, as in figure 1.

Since we have obtained the simple expression (3.5) for $X(f)$ by integration, the

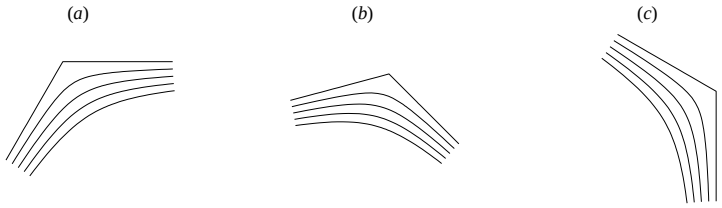

Figure 1. Sample exact free-surface flows with $X \propto Y \propto f^{2/3}$: (*a*) $B \to 0$, $C \to \infty$; (*b*) $0 < B < (g/2g)^{1/3}$, $\infty > C > 0$; (*c*) $B = (g/2g)^{1/3}$, $C = 0$.

simple expression (3.1) for $Y(f)$ can be retrieved by solving the differential equation (2.5) with that choice of $X(f)$, i.e.

$$\left(\frac{\mathrm{d}Y}{\mathrm{d}f}\right)^2 + \frac{1}{2gY} = -\frac{4}{g}C^2 f^{-2/3}. \tag{3.8}$$

It is indeed clear by inspection that (3.1) is the solution of (3.8) satisfying the initial condition

$$Y = 0 \text{ at } f = 0, \tag{3.9}$$

providing B and C are connected by (3.4). However, it is not as obvious what is the solution of (3.8) subject to any other initial condition; in recent unpublished work, we have obtained the general solution of (3.8), but have not identified any useful special cases other than (3.1). In particular, the solution subject to $Y(0) = A$ is *not* $Y = A - Bf^{2/3}$.

But in any case, let us pursue the choice

$$Y(f) = A - Bf^{2/3}, \tag{3.10}$$

for some constant A. Then (2.2) gives

$$\begin{aligned} X'^2 &= -\frac{4}{9}B^2 f^{-2/3} - \frac{1}{2g}\left(A - Bf^{2/3}\right)^{-1} \\ &= -\frac{1}{2g}\left[\left(1 - \tfrac{8}{9}gB^3\right) + \tfrac{8}{9}gB^2 A f^{-2/3}\right]\left(A - Bf^{2/3}\right)^{-1}. \end{aligned} \tag{3.11}$$

We integrate (3.11) in the general case later; meanwhile let us note the interesting special case

$$B = (9/8g)^{1/3}. \tag{3.12}$$

The requirement that X and Y be simultaneously real on $\psi = 0$ can be met only if $A \geqslant 0$ and $\phi > (A/B)^{3/2}$, that is $Y < 0$. Now if (3.12) holds, (3.11) integrates to

$$X = 2A^{1/2}\left(Bf^{2/3} - A\right)^{1/2} \tag{3.13}$$

$$\Rightarrow \quad z = 2(-AY)^{1/2} + \mathrm{i}Y, \tag{3.14}$$

where Y is given by (3.10). The free surface is the parabola

$$y = -\frac{1}{4A}x^2. \tag{3.15}$$

In fact, it is easy to show that fluid particles on this parabolic free-surface streamline are falling freely in a true ballistic trajectory with a constant horizontal velocity of magnitude $(g/8A)^{1/2}$.

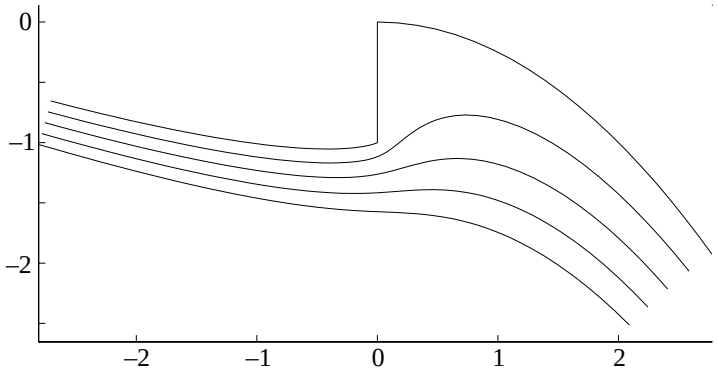

Figure 2. Bow flow (3.16) showing the vertical front of the bow, the 240° submerged corner, and the parabolic free-surface. Plotted here, and in the subsequent figures, are the streamlines $\psi = -(0 : 0.5 : 2)$ for a potential range of approximately $-15 < \phi < 5$.

The free surface is the portion $\phi > (A/B)^{3/2}$ of the streamline $\psi = 0$. The portion $0 < \phi < (A/B)^{3/2}$ is a vertical wall $x = 0$ since (3.14) implies that z is pure imaginary in this range. This wall extends from the origin down to $Y = -A$, at which point there is a 240° corner flow, i.e. the flow direction changes suddenly from vertical to 30° to the horizontal downward. For $\phi < 0$, there is a curved body shape, and as $\phi \to -\infty$, this body asymptotes to a 30° upward straight line.

Figure 2 shows the flow, in non-dimensional form, noting that if $Z = z/A$ and $F = (A/B)^{3/2} f$, (3.14) becomes just

$$Z = 2\left(-1 + F^{2/3}\right)^{1/2} + \mathrm{i}\left(1 - F^{2/3}\right). \tag{3.16}$$

In effect, all solutions of this type are recoverable by rescaling the solution with $A = B = 1$, $g = \frac{9}{8}$.

Even when (3.12) does not hold, closed-form integration of (3.11) is possible. For example, if A and B are both positive, then

$$X = \left(\frac{1-\gamma}{\gamma}\right)^{1/2} \left\{ [-Y(K-Y)]^{1/2} + K \log\left[\frac{(-Y)^{1/2} + (K-Y)^{1/2}}{K^{1/2}}\right]\right\}, \tag{3.17}$$

where

$$\gamma = \tfrac{8}{9} g B^3, \tag{3.18}$$

and

$$K = \frac{A}{1-\gamma}. \tag{3.19}$$

Again, a normalization equivalent to setting $A = B = 1$ may be performed. The solution (3.17) is most straightforward to use if $\gamma < 1$; note that the limit $\gamma \to 1$ ($K \to \infty$) reproduces the solution (3.13).

As an example, figure 3 shows the solution for $\gamma = 3/4$ ($K = 4$). This is a case where the body's lower surface is asymptotically *horizontal* as $\phi \to -\infty$. This flow models (to a limited extent) a finite-draft semi-infinite bow or stern flow for a ship. However, there is no streaming flow at infinity, and the free surface slopes downward at 60° to the horizontal.

More generally, all members of the family (3.17) have (in the notation of § 1)

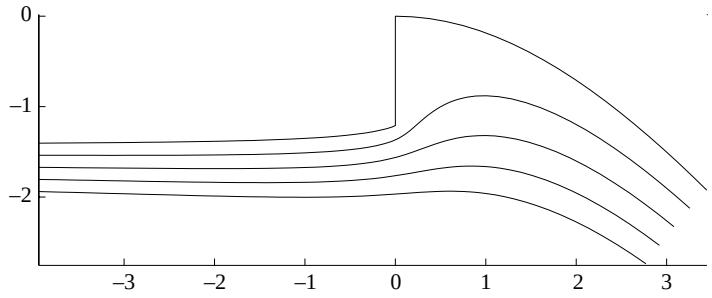

Figure 3. Bow flow (3.17) showing the solid body's lower surface to be asymptotically horizontal.

$\tan\theta = -\sqrt{\gamma/(1-\gamma)}$ and (2.7) holds. All members have a body containing a vertical wall, where the free surface joins the body, with a 240° corner at its bottom end, followed by a curved bottom that asymptotes to a line at 120° to the free surface.

There is an apparent singularity in (3.17) where $Y = K$; however, for $\gamma < 1$, so $K > 0$, this singularity is not in the region of flow. In general, such a singularity must be expected wherever X'^2 possesses a *simple* zero, and many otherwise plausible choices for $Y(f)$ are unacceptable because of this difficulty.

All flows in the present section are such that the far-field has z as a two-thirds power of f, or equivalently are such that the velocity at infinity increases like the one-half power of distance. This they have in common with the splashing flow of Jenkins (1994) and the flows studied by Vanden-Broeck & Tuck (1994). This being so, they are not yet capable of immediate application to ship bow flows, where we would prefer a finite uniform stream at infinity. As a first step toward the latter objective, let us now examine other power-law flows.

4. Y as a power of X

Inspired by the solution (3.14) in which the free surface is given by the simple parabolic equation (3.15), we seek solutions of (2.2) for which the free surface has a power law dependence, namely $y = -Ax^\beta$. Thus we look for solutions of the form

$$z = X - \mathrm{i}AX^\beta, \tag{4.1}$$

where $X(f)$ is real on the free surface $\psi = 0$, $\phi > 0$. In fact this is a special case of a procedure discussed by Wilton (1913) and Wehausen & Laitone (1960) enabling solution with an arbitrary given form for the free surface.

Substituting (4.1) into (2.2) we find that X must be given by the following integral

$$f = \sqrt{2gA}\int X^{\beta/2}\sqrt{1 + A^2\beta^2X^{2\beta-2}}\,\mathrm{d}X, \tag{4.2}$$

or, upon substituting

$$\xi = A\beta X^{\beta-1}, \tag{4.3}$$

by

$$f = B\int \xi^n\sqrt{1+\xi^2}\,\mathrm{d}\xi, \tag{4.4}$$

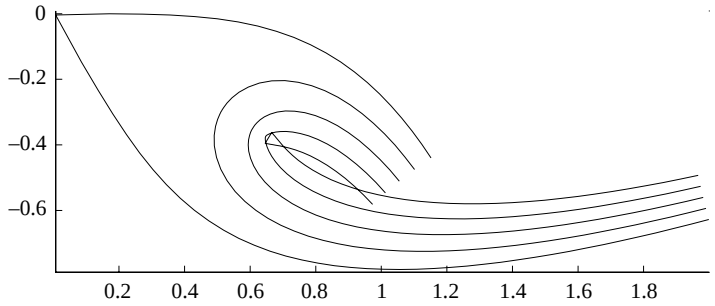

Figure 4. Bow flow (4.1) for $n = 0$, $\beta = 4$ showing an unreasonable singularity in the fluid somewhere in $-2 < \psi < -1.5$.

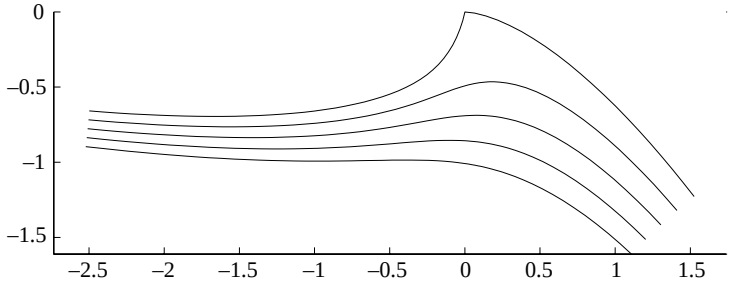

Figure 5. Bow flow (4.1) for $n = 2$, $\beta = 8/5$.

where

$$B^2 = \frac{2g}{\beta(\beta-1)^2(\beta A)^{3/(\beta-1)}}, \tag{4.5}$$

and

$$n = \frac{(4-\beta)}{2(\beta-1)}. \tag{4.6}$$

In fact, the problem can be non-dimensionalized to assign any convenient value to B and A; we choose $B = n + 2$ and $A = |\beta|^{-1}$ in the following examples.

For integer n, the integral in (4.4) can be written down explicitly, for example:

$$n = 0,\ \beta = 4: \quad \xi = X^3, \quad f = \sinh^{-1}(\xi) + \xi\sqrt{1+\xi^2}, \tag{4.7}$$

$$n = 1,\ \beta = 2: \quad \xi = X, \quad f = (1+\xi^2)^{3/2}, \tag{4.8}$$

$$n = 2,\ \beta = \tfrac{8}{5}: \quad \xi = X^{3/5}, \quad f = -\tfrac{1}{2}\sinh^{-1}(\xi) + (\tfrac{1}{2}+\xi^2)\xi\sqrt{1+\xi^2}, \tag{4.9}$$

$$n = 3,\ \beta = \tfrac{10}{7}: \quad \xi = X^{3/7}, \quad f = (-\tfrac{2}{3}+\xi^2)(1+\xi^2)^{3/2} \tag{4.10}$$

etc. These flows are depicted in figures 4, 2, 5 and 6, respectively.

Observe that the $n = 1$ flow is precisely a flow already examined in the previous section; thus this family of solutions generalizes that solution. The $n = 0$ flow is inappropriate as a bow flow as it involves a singularity in the fluid flow. The $n = 2$ and 3 flows can model a bow flow where the bow profile intersects with the horizontal free-surface at an angle of $\frac{5}{9}\pi$ and $\frac{7}{12}\pi$, respectively.

These flows are clearly isolated examples of a one parameter family of solutions

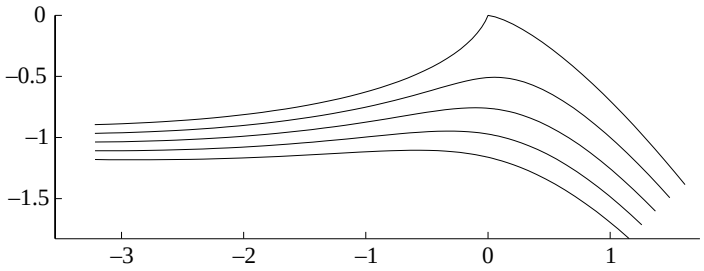

Figure 6. Bow flow (4.1) for $n = 3$, $\beta = 10/7$.

given by β varying from 1 to ∞. The general characteristics of this family are that they possess a bow-like corner flow, the bow being inclined at an angle $2\pi/(\beta + 2)$ to the asymptotically horizontal free surface. In the far field, the free surface is asymptotically vertical, whereas the solid body asymptotes to a line inclined at an upward angle of 30° to the horizontal. The singularity at $\xi = -\mathrm{i}$ in (4.4) is outside the flow for $\beta < 2$, has moved to be exactly on the body if $\beta = 2$, and moves into the flow for $\beta > 2$. Thus, acceptable solutions only occur for $1 < \beta \leqslant 2$, which corresponds to $n \geqslant 1$. As $\beta \to 1^+$ (large n) the flow tends to the 2/3 power flow (3.6) discussed earlier.

5. Differential equation

A little used approach to finding solutions to (2.2) is to write it in the form (2.5) which, given a specified $X(f)$, is a first-order differential equation for $Y(f)$. In conjunction with this differential equation the initial condition

$$Y(0) = 0, \tag{5.1}$$

will be used throughout this section. The more general possibility of $Y(0) = K < 0$ is not considered.

We also consider only that class of flows obtained by choosing

$$X(f) = \lambda f^{\alpha}, \quad 0 < \alpha \leqslant 1. \tag{5.2}$$

On its own this represents a flow in a corner of angle $\alpha\pi$ radians, and we hope that this character will hold in the full solution and so represent a bow flow where the angle which the profile of the bow makes with the horizontal is $\alpha\pi$ radians. In fact, this is true provided $0 < \alpha < \frac{2}{3}$ which will thus be the main range of α investigated.

Now, by scaling f, X and Y appropriately we can in effect set

$$g = \tfrac{1}{2} \quad \text{and} \quad A = 1/\alpha, \tag{5.3}$$

which gives a one parameter family of differential equations to solve. That is, if we find $Y(f)$ such that

$$\left(\frac{\mathrm{d}Y}{\mathrm{d}f}\right)^2 + \frac{1}{Y} + f^{2\alpha-2} = 0, \tag{5.4}$$

subject to the initial condition (5.1), then the inverse complex potential

$$Z(f) = \frac{1}{\alpha} f^{\alpha} + \mathrm{i}Y(f), \tag{5.5}$$

represents a fluid flow with a free surface whenever f is real, $f > 0$ and $Y(f)$ is real.

The only known analytic solutions to (5.4) are the cases $\alpha = 1$ (see Vitousek 1954) and $\alpha = \frac{2}{3}$ (see § 2). For general α we resort to a numerical solution; for example, see Vanden-Broeck *et al.* (1978) where the case $\alpha = \frac{1}{2}$ is investigated.

(*a*) *Asymptotic behaviour*

It is helpful to obtain a rough picture of the behaviour of the solutions of this problem. To do this, the asymptotic behaviour as $f \to 0$ and as $f \to \infty$ is given here.

First consider the range $0 < \alpha < \frac{2}{3}$. As $f \to 0$ the $\mathrm{d}Y/\mathrm{d}f$ term in (5.4) is negligible and hence

$$Z(f) \sim (1/\alpha) f^{\alpha} - \mathrm{i} f^{2-2\alpha}, \quad f \to 0, \tag{5.6}$$

which is a flow in a corner of $\alpha\pi$ radians, as desired, but modified by the second term. In particular, this second term shows that the free surface is

$$y \sim -(\alpha x)^{2(1-\alpha)/\alpha}, \quad x \to 0^{+}. \tag{5.7}$$

As $f \to \infty$, the $f^{2\alpha-2}$ term in (5.5) is negligible and hence

$$Z(f) \sim -\mathrm{i}\left(\tfrac{3}{2} f\right)^{2/3} + \frac{1}{\alpha} f^{\alpha}, \quad f \to \infty, \tag{5.8}$$

which is flow in a 120° corner (modified by the f^{α} term) with the free surface vertically downwards and the boundary of the solid body (f real and $f < 0$) to the left and inclined 30° upwards from the horizontal. Thus in this range of α, the behaviour of all solutions of the ODE (5.4) should be much like those given in the preceding section (with α corresponding to $2/(\beta + 2)$).

Now consider the range $\frac{2}{3} < \alpha < 1$. As $f \to 0$, the $f^{2\alpha-2}$ term in (5.4) is negligible and hence

$$Z(f) \sim -\mathrm{i}\left(\tfrac{3}{2} f\right)^{2/3} + \frac{1}{\alpha} f^{\alpha}, \quad f \to 0, \tag{5.9}$$

which is a flow in a corner of 120° with the free surface asymptotically vertical. As $f \to \infty$, the $\mathrm{d}Y/\mathrm{d}f$ term is not negligible and hence

$$Z(f) \sim \frac{1}{\alpha} f^{\alpha} - \mathrm{i} f^{2-2\alpha}, \quad f \to \infty, \tag{5.10}$$

which is the requisite corner flow of $\alpha\pi$ radians but in this case it only occurs in the far field and so is of less interest as a model of bow flow.

(*b*) *Numerical integration*

To solve (5.4) numerically, we write it as

$$\frac{\mathrm{d}Y}{\mathrm{d}f} = \left[-\frac{1}{Y} - f^{2\alpha-2}\right]^{1/2}, \tag{5.11}$$

and then use a variable-step Runge–Kutta integration scheme to find $Y(f)$ along any path in the complex f-plane which starts at the initial point $f = 0$. In particular, integration along constant ϕ or ψ lines are of interest, as these give equipotentials and streamlines, respectively.

However, the initial condition (5.1) cannot be applied precisely, as the right hand side of (5.11) is singular there. Thus the integration is commenced at some small real

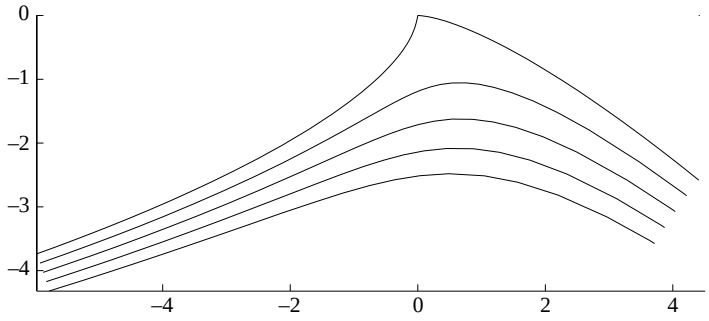

Figure 7. Flow obtained by solving the ODE for $\alpha = 0.55$.

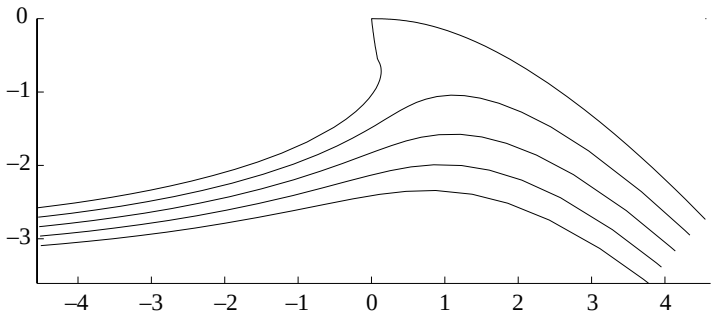

Figure 8. Flow obtained by solving the ODE for $\alpha = 0.463$.

positive f, with $Y(f)$ being given by an asymptotic series (the first term of which is given in (5.6)). Furthermore, in order to maintain accuracy, the path of integration must not get too close to the origin and hence should start away from the origin, preferably along the real axis (that is, on the free surface).

The square root in (5.11) is evaluated so that it is initially real and negative and then as the integration proceeds the correct branch is chosen by requiring that $\mathrm{d}Y/\mathrm{d}f$ be continuous.

By the above procedure we obtain the solutions shown in figures 7 ($\alpha = 0.55$) and 8 ($\alpha = 0.463$). Vanden Broeck *et al.* (1978) used similar tactics to solve the case when $\alpha = 1/2$. The flows are qualitatively similar to the analytic solutions described in the previous section. An interesting case is $\alpha = 0.463$, where the solid body possesses an underwater bulge reminiscent of the bow-shape of large ocean going vessels.

(*c*) *Singularities*

For values of α significantly less than $\frac{1}{2}$, say $\alpha = \frac{1}{4}$, the numerical integration of (5.4) shows that some streamlines cross. Furthermore, there exist closed paths of integration lying in $Y < 0$ for which the corresponding path in the Z-plane is open. Both these facts show that there is a singularity in $Y(f)$ for $\psi < 0$. Since the singularity must be excluded from the fluid flow, ψ can no longer extend to $-\infty$. This trait is again very similar to some of the solutions in the previous section.

However, determining the value of α at which the singularity moves into the fluid flow is much more difficult here. First, we make the transformation

$$Y(f) = -f^{2/3}u(\eta), \tag{5.12}$$

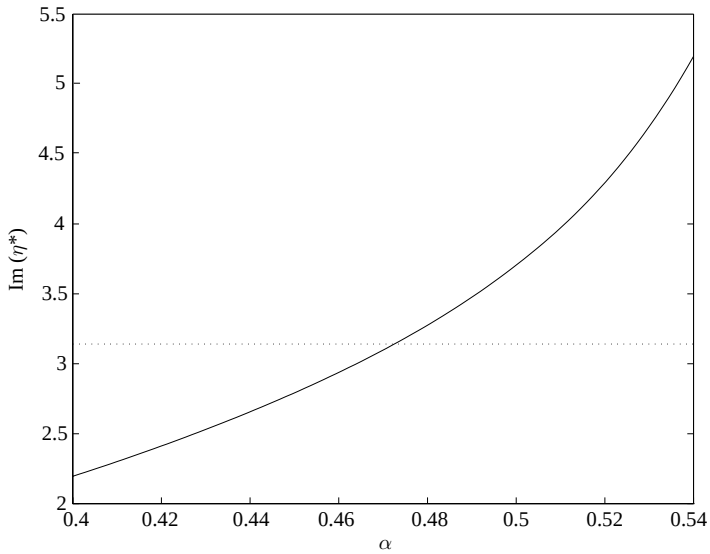

Figure 9. A plot of $-\mathrm{Im}(\eta^*)$ versus the parameter α, where η^* is the location of a singularity in the complex η-plane. When, at about $\alpha = 0.462$, $\mathrm{Im}(\eta^*)$ crosses $-\pi$, the singularity moves into the fluid flow field.

$$\eta = \log f, \tag{5.13}$$

and find that $u(\eta)$ must satisfy

$$\frac{1}{u} - \left(\frac{2}{3}u + \frac{\mathrm{d}u}{\mathrm{d}\eta}\right)^2 = \mathrm{e}^{2(\alpha-2/3)\eta}. \tag{5.14}$$

Second, we numerically integrate (5.11) as accurately as possible to some real $f_0 = \mathrm{e}^{\eta_0}$ to obtain an accurate value for $u_0 = u(\eta_0)$. Then we calculate the Taylor series of u as a function of η about the point η_0 using the differential equation (5.14). Typically, up to 30 coefficients in the Taylor series could be found before numerical error became significant (using $\eta_0 = 0$ and $\eta_0 = 1$).

The transformation (5.13) maps the singularity due to the stagnation point at $f = 0$ to infinity in the η-plane and so the Taylor series of $u(\eta)$ will now have its radius of convergence limited by the nearest singularity to η_0 in the η-plane. The position and nature of this singularity may be found by an extension (described in the Appendix of the paper by Mercer & Roberts 1990) of the procedure of Domb & Sykes (1957). Plotted in figure 9 is the result of interest, namely the value of $-\arg(f^*)$ at which a singularity occurs (i.e. the imaginary part of η^*). Since the fluid domain corresponds to $-\pi < \arg(f) \leqslant 0$, this figure shows that for $\alpha > 0.462$ the singularity is outside the fluid domain, but for $\alpha < 0.462$ it has moved through the body and into the fluid.

There may be other singularities in the fluid domain, but none were detected in the numerical integration. Thus, bow-like flows can be found for bows at a lesser angle than 90° to the horizontal, here down to 83°.

References

Cumberbatch, E. 1958 Two-dimensional planing at high Froude number. *J. Fluid Mech.* **4**, 466–478.

Dias, F. & Tuck, E. O. 1993 A steady breaking wave. *Phys. Fluids* **5**, 277–279.

Dias, F. & Vanden-Broeck, J.-M. 1993 Nonlinear bow flows with spray. *J. Fluid Mech.* **255**, 91–102.

Domb, C. & Sykes, M. F. 1957 On the susceptibility of a ferromagnet above the Curie point. *Proc. R. Soc. Lond.* A **240**, 214–228.

Farrow, D. E. & Tuck, E. O. 1995 Further studies of stern wavemaking. *J. Aust. Math. Soc.* B **36**, 424–437.

Jenkins, A. D. 1994 A stationary potential-flow approximation for a breaking-wave crest. *J. Fluid Mech.* **280**, 335–347.

Madurasinghe, D. A. M. 1988 Splashless ship bows with stagnant attachment. *J. Ship Res.* **32**, 194–202.

Madurasinghe, D. A. M. & Tuck, E. O. 1986 Ship bows with continuous and splashless attachment. *J. Aust. Math. Soc.* B **27**, 442–452.

Mercer G. N. & Roberts, A. J. 1990 A centre manifold description of contaminant dispersion in channels with varying flow properties. *SIAM Jl Appl. Math.* **50**, 1547–1565.

Mori, K. H. 1984 Necklace vortex and bow wave around blunt bodies. *Proc. 15th ONR Symp. Naval Hydro. Hamburg.* Washington DC: Nat. Acad. Press.

Newman, J. N. 1977 *Marine hydrodynamics.* Cambridge, MA: MIT Press.

Raven, H. 1992 A practical nonlinear method for calculating ship wavemaking and wave resistance. *Proc. 19th ONR Symp. Naval Hydro.* Seoul, Korea.

Roberts, A. J. 1987 Transient free-surface flows generated by a moving vertical plate. *Q. Jl Mech. Appl. Math.* **40**, 129–158.

Sautreaux, C. 1901 Mouvement d'un liquide parfait soumis a la pesanteur. Determination des lignes de courant. *J. Math. Pures Appl.* **7**, 125–159.

Scullen, D. & Tuck, E. O. 1995 Nonlinear free-surface flow computations for submerged cylinders. *J. Ship Res.* **39**, 185–193.

Tuck, E. O. 1991 Ship-hydrodynamic free-surface problems without waves. *J. Ship Res.* **35**, 277–287.

Tuck, E. O. 1994 The planing splash. *Proc. 9th Int. Workshop on Water Waves and Floating Bodies* (ed. M. Ohkusu). Kyushu University, Japan.

Tuck, E. O. 1995 Planing surfaces. *Proc. A. C. Aitken Centenary Conference.* University of Otago, Dunedin, NZ.

Tuck, E. O. 1997 Ploughing flows. *Euro. J. Appl. Math.* (In the press.)

Tuck, E. O. & Vanden-Broeck J.-M. 1984 Splashless bow flows in two dimensions? *Proc. 15th ONR Symp. Naval Hydro. Hamburg.* Washington DC: Nat. Acad. Press.

Vanden-Broeck J.-M., Schwartz, L. W. & Tuck, E. O. 1978 Divergent low-Froude-number series expansion of nonlinear free-surface flow problems. *Proc. R. Soc. Lond.* A **361**, 207–224.

Vanden-Broeck J.-M. & Tuck, E. O. 1994 Flow near the intersection of a free surface with a vertical wall. *SIAM Jl Appl. Math.* **54**, 1–13.

Vitousek, M. J. 1954 Some flows in a gravity field satisfying the exact free surface condition. *Stanford University Tech. Report* **25**, 287.

Wehausen, J. V. & Laitone, E. V. 1960 Surface waves. In *Handbuch der Physik* (ed. S. Flugge), vol. 8. Berlin: Springer.

Wilton, J. R. 1913 On the highest wave in deep water. *Phil. Mag.* **26**, 1053–1058.